Soil erosion by snow gliding – a first quantification attempt in a sub-alpine area, Switzerland

K. Meusburger[1], G. Leitinger[2], L. Mabit[3], M. H. Mueller[1], A. Walter[1] and C. Alewell[1]

[1] Environmental Geosciences, University of Basel, Basel, Switzerland

[2] Institute of Ecology, University of Innsbruck, Innsbruck, Austria

[3] Soil and Water Management & Crop Nutrition Laboratory, Joint FAO/IAEA Division of Nuclear Techniques in Food and Agriculture, International Atomic Energy Agency, Austria

Abstract

Snow processes might be one important driver of soil erosion in Alpine grasslands and thus the unknown variable when erosion modelling is attempted. The aim of this study is to assess the importance of snow gliding as soil erosion agent for four different land use/land cover types in a sub-alpine area in Switzerland. We used three different approaches to estimate soil erosion rates: sediment yield measurements in snow glide depositions, the fallout radionuclide ^{137}Cs, and modelling with the Revised Universal Soil Loss Equation (RUSLE). RUSLE permits the evaluation of soil loss by water erosion, the ^{137}Cs method integrates soil loss due to all erosion agents involved, and the snow glide deposition sediment yield measurement can be directly related to snow glide induced erosion. Further, cumulative snow glide distance was measured for the sites in the winter 2009/2010 and modelled for the surrounding area and long-term average winter

precipitation (1959-2010) with the Spatial Snow Glide Model (SSGM). Measured snow glide distance confirmed the presence of snow gliding and ranged from 2 to 189 cm, with lower values at the north facing slopes. We observed a reduction of snow glide distance with increasing surface roughness of the vegetation, which is important information with respect to conservation planning and expected and ongoing land use changes in the Alps. Snow glide erosion estimated from the snow glide depositions was highly variable with values ranging from 0.03 to 22.9 t ha^{-1} yr^{-1} in the winter 2012/2013. For sites affected by snow glide deposition, a mean erosion rate of 8.4 t ha^{-1} yr^{-1} was found. The difference in long-term erosion rates determined with RUSLE and ^{137}Cs confirm the constant influence of snow glide induced erosion, since a large difference (lower proportion of water erosion compared to total net erosion) was observed for sites with high snow glide rates and vice versa. Moreover, the difference of RUSLE and ^{137}Cs erosion rates was related to the measured snow glide distance (R^2 = 0.64; $p<0.005$) and to the snow deposition sediment yields (R^2 = 0.39; p = 0.13). The SSGM reproduced the relative difference of the measured snow glide values under different land uses and land cover types. The resulting map highlighted the relevance of snow gliding for large parts of the investigated area. Based on these results, we conclude that snow gliding appears to be a crucial and non-negligible process impacting soil erosion pattern and magnitude in sub-alpine areas with similar topographic and climatic conditions.

Keywords: soil erosion, Alps, snow, ^{137}Cs, RUSLE

1 Introduction

While rainfall is a well-known agent of soil erosion, the erosive forces of snow movements are qualitatively recognized but quantification has not been achieved yet (Leitinger et al., 2008; Konz et al., 2012). Particularly wet avalanches can yield enormous erosive forces that are responsible for major soil loss (Gardner, 1983; Ackroyd, 1987; Bell et al., 1990; Jomelli and Bertran, 2001; Heckmann et al., 2005; Fuchs and Keiler, 2008; Freppaz et al., 2010) also in the avalanche release area (Ceaglio et al., 2012).

Besides avalanches another important process of snow movement affecting the soil surface is snow gliding (In der Gand and Zupancic, 1966). Snow gliding is the slow (mm to cm per day) downhill motion of a snowpack over the ground surface caused by the stress of its own weight (Parker, 2002). Snow gliding predominantly occurs on south-east to south-west facing slopes with slope angles between 30-40° (In der Gand and Zupancic, 1966; Leitinger et al., 2008). Two main factors that control snow glide rates are (i) the wetness of the boundary layer between the snow and soil cover and (ii) the ground surface roughness determined by the vegetation cover and rocks (McClung and Clarke, 1987; Newesely et al., 2000). So far, only few studies investigated the effect of snow gliding on soil erosion (Newesely et al., 2000; Leitinger et al., 2008). A major reason for this shortcoming is the difficulty to obtain soil erosion rates caused by snow processes. In steep sub-alpine areas soil erosion records (e.g. with sediment traps) are restricted to the vegetation period because avalanches and snow gliding can irreversibly damage the experimental design (Konz et al., 2012).

Recently, first physically based attempts to model the erosive force of wet avalanches were done (Confortola et al., 2012). No similar model exists for snow

77 gliding. However, the potential maximum snow glide distance during a targeted
78 period can be modelled with the empirical Spatial Snow Glide Model (SSGM)
79 (Leitinger et al., 2008). The modelling of this process is crucial to evaluate the
80 impact of the snow glide process on soil erosion at larger scale.
81 Soil erosion rates can be obtained by direct quantification of sediment transport
82 in the field, by fallout radionuclides (FRN) based methods (e.g. Mabit et al.,
83 1999; Benmansour et al., 2013; Meusburger et al., 2013) and by soil erosion
84 models (Nearing et al., 1989; Merritt et al., 2003). Since the end of the 1970's
85 empirical soil erosion models such as the Universal Soil Loss Equation (USLE;
86 Wischmeier and Smith, 1965; Wischmeier and Smith, 1978), and its refined
87 versions the Revised USLE (RUSLE; Renard et al., 1997) and the Modified USLE
88 (MUSLE; Smith et al., 1984), have been used worldwide to evaluate soil erosion
89 magnitude under various conditions (Kinnell, 2010). These well-known models
90 allow the assessment of sheet erosion and rill/inter-rill erosion under moderate
91 topography. However, they do not integrate erosion processes associated with
92 wind, mass movement, tillage, channel or gully erosion (Risse et al., 1993; Mabit
93 et al., 2002; Kinnell, 2005) and also snow impact due to movement is not
94 considered (Konz et al., 2009). Several models have been tested for steep alpine
95 sites with the result that RUSLE reproduced the magnitude of soil erosion, the
96 relative pattern and the effect of the vegetation cover most plausible (Konz et
97 al., 2010; Meusburger et al., 2010b; Panagos et al., 2014). The erosion rate
98 derived from RUSLE corresponds to water erosion induced by rainfall and surface
99 runoff and hence in our site to the soil erosion processes during the summer
100 season without significant influence of snow processes.
101 In contrast, the translocation of FRN reflects all erosion processes by water, wind
102 and snow during summer and winter season and thus, is an integrated estimate
103 of the total net soil redistribution rate since the time of the fallout in the 1950s

(the start of the global fallout deposit) and in case of predominant Chernobyl ^{137}Cs input since 1986. Anthropogenic fallout radionuclides have been used worldwide since decades to assess the magnitude of soil erosion and sedimentation processes (Mabit and Bernard, 2007; Mabit et al., 2008; Matisoff and Whiting, 2011). The most well-known conservative and validated anthropogenic radioisotope used to investigate soil redistribution and degradation is ^{137}Cs (Mabit et al., 2013).

For (sub-) alpine areas the different soil erosion processes captured by RUSLE and the ^{137}Cs method result in different erosion rates (Konz et al., 2009; Juretzko, 2010; Alewell et al., 2014; Stanchi et al., 2014, accepted). However, this difference might also be due to several other reasons such as the error of both approaches, the non-suitability of the RUSLE model for this specific environment and/or the erroneous estimation of the initial fallout of ^{137}Cs.

In this study, we aim to quantify snow glide induced erosion and investigate, whether the observed discrepancy between erosion rates estimated with RUSLE and the ones provided by the ^{137}Cs method can be at least partly attributed to snow gliding processes. Since vegetation cover affects snow gliding, four different sub-alpine land use/land cover types were investigated. A further objective of our research is to assess the relevance of snow gliding processes at catchment scale using the Spatial Snow Glide Model (SSGM).

2 Materials and Methods

2.1 Site description

The study site is located in Central Switzerland (Canton Uri) in the Ursern Valley (Fig. 1). The elevation of the W–E extended alpine valley ranges from 1400 up to 2500 m a.s.l. At the valley bottom (1442 m a.s.l.), average annual air temperature for the years 1980–2012 is around 4.1 ± 0.7 °C and the mean annual

precipitation is 1457 ± 290 mm, with 30% falling as snow (MeteoSwiss, 2013). The valley is snow covered from November to April with a mean annual snow height of 67cm in the period 1980 to 2012. Drainage of the basin is usually controlled by snowmelt from May to June. Important contribution to the flow regime takes place during early autumn floods. The land use is characterised by hayfields near the valley bottom (from 1450 to approximately 1650 m a.s.l.) and pasturing further upslope. Siliceous slope debris and moraine material is dominant at our sites, and forms Cambisols (Anthric) and Podzols (Anthric) classified after IUSS Working Group (2006).

Of the 14 experimental sites, 9 are located at the south-facing slope and 5 at the north-facing slope at altitudes between 1476 and 1670 m a.s.l. Four different land use/cover types with 3-5 replicates each were investigated: hayfields (h), pastures (p), pastures with dwarf shrubs (pw), and abandoned grassland covered with *Alnus viridis* (A). Vegetation of hayfields is dominated by *Trifolium pratense*, *Festuca sp.*, *Thymus serpyllum* and *Agrostis capillari~~e~~s*. For the pastured grassland *Globularia cordifolia*, *Festuca sp.* and *Thymus serpyllum* dominate. Pastures with dwarf shrubs are dominated by *Calluna vullgaris*, *Vaccinium myrtillus*, *Festuca violacea*, *Agrostis capillari~~e~~s* and *Thymus serpyllum*. At pasture sites of the south facing slope, which are stocked from June to September, cattle trails transverse to the main slope direction.

2.2 Snow glide measurement

We measured cumulative snow glide distances with snow glide shoes for the winter 2009/2010. The snow glide shoe equipment was similar to the set-up used by In der Gand and Zupancic (1966), Newesely et al. (2000) and Leitinger et al. (2008). The set-up consisted of a glide shoe and a buried weather-proof box with a wire drum. Displacement of the glide shoe causes the drum to unroll the

wire. The total unrolled distance was measured in spring after snowmelt. To prevent entanglement with the vegetation, the steel wire was protected by a flexible plastic tube. For each site, 3 to 5 snow glide shoes were installed to obtain representative values. A total of 60 devices were used.

2.3 Assessment of soil redistribution

Snow glide distance was measured with snow glide shoes for 14 sites. For 12 of the 14 sites (exclusive of the two *Alnus viridis* sites at the north facing slopes (AN)), RUSLE and ^{137}Cs based erosion rates were assessed. Seven of these sites were measured in 2007 (Konz et al., 2009). During a second field campaign performed in 2010, 5 additional sites were investigated using the same methods for soil erosion assessment with ^{137}Cs and RUSLE as in 2007 (Konz et al., 2009). The ^{137}Cs measurements were decay corrected to 2007 for comparison purpose.

2.3.1 Snow and sediment sampling in the snow glide deposition area

Sediment concentrations were estimated by measuring the amount of sediment in snow samples taken with a corer from the snow glide depositions in spring 2013 (Fig. 2). The corer allowed for the sampling of the entire depth of the snow deposition and thus the integration of the sediment yield over the depth of the deposition. For larger depositions, samples were collected along two transects across each deposition. For smaller depositions, we took three samples. The samples were melted and filtered through a 0.11 µm filter. The filtered material was dried at 40°C and weighted to obtain the concentration of sediment per sample (M_S). The mean sediment values (and for depositions with several samples the interpolated mean sediment values) were used to estimate the total sediment load of the snow-glide deposition (M_A) according to:

$$M_A = \frac{A_A \times M_S}{A_c} \qquad \textbf{Equation 1}$$

where A_c is the area of the corer and A_A is the area of the snow-glide deposition. The latter was mapped in the field by GPS and measuring tape. Sediment load was further converted to soil erosion rate (E) by:

$$E = \frac{M_A}{A_S} \qquad \textbf{Equation 2}$$

where A_s is the source area of the snow and sediment deposition. Each snow glide was photo documented and the respective source area was mapped with GPS and transferred to ArcGIS for surface area estimation.

2.3.2 Assessment of soil redistribution by water erosion using the RUSLE

The USLE (Wischmeier and Smith, 1978) and its revised version the RUSLE (Renard et al., 1997) is an empirical erosion model originally developed in the United States. Several adapted versions for other regions as well as for different temporal resolutions have been developed and applied with more or less success (Kinnell, 2010). Despite its well-known limitation (highlighted in our introduction), we selected RUSLE because of the lack of simple soil erosion models specific for mountain areas and moreover because of its better performance when compared to the other existing models (Konz et al., 2010; Meusburger et al., 2010b). The RUSLE can be calculated using the following equation:

$$A = R \times K \times LS \times C \times P \qquad \textbf{Equation 3}$$

where A is the predicted average annual soil loss (t ha^{-1} yr^{-1}). R is the rainfall-runoff-erosivity factor (N h^{-1}) that quantifies the effect of raindrop impact and reflects the rate of runoff likely to be associated with the rain (Renard et al., 1997). The soil erodibility factor K (N h kg m^{-2}) reflects the ease of soil

206 detachment by splash or surface flow. The parameter *LS* (dimensionless)
207 accounts for the effect of slope length (*L*) and slope gradient (*S*) on soil loss. The
208 *C*-factor is the cover factor, which represents the effects of all interrelated
209 cover and management variables (Renard et al., 1997).
210 For comparability between the RUSLE estimates of Konz et al. (2009) and the
211 ones assessed in this study we used the same R-factor approximation of Rogler
212 and Schwertmann (1981) adapted by Schuepp (1975). According to the USLE
213 procedure, snowmelt can be integrated in erosivity calculation by multiplying
214 snow precipitation by 1.5 and then adding the product to the kinetic energy
215 times the maximum 30-min intensity. However, the latter procedure does not
216 account for redistribution of snow by drifting, sublimation, and reduced
217 sediment concentrations in snowmelt (Renard et al., 1997). Therefore, as
218 suggested by Renard (1997) this adaption of the R-factor was not considered in
219 this study. The K-factor was calculated with the K nomograph after Wischmeier
220 and Smith (1978) using grain-size analyses and carbon contents of the upper 15
221 cm of the soil profiles. Total C content of soils was measured with a Leco CHN
222 analyzer 1000, and grain size-analyses were performed with sieves for grain sizes
223 between 32 and 1000 µm and with a Sedigraph 5100 (Micromeritics) for grain
224 sizes between 1 and 32 µm. L and S were calculated after Renard et al. (1997).
225 The support and practice factor P (dimensionless) was set to 0.9 for some of the
226 pasture sites because alpine pastures with cattle trails resemble small terrace
227 structures, which are suggested to be considered in P (Foster and Highfill, 1983).
228 For all other sites, P value was set to 1. The cover-and-management factor C
229 was assessed for sites with and without dwarf shrubs separately using measured
230 fractional vegetation cover (FVC) in the field.
231 For investigated sites without dwarf shrubs (US Department of Agriculture,
232 1977)~~(US Department of Agriculture, 1977)~~ the C-factor can be estimated with:

$$C = 0.45 \times e^{-0.0456 \times FVC} \quad \textbf{Equation 4}$$

and for sites with dwarf shrubs the following equation was used:

$$C = 0.45 \times e^{-0.0324 \times FVC} \quad \textbf{Equation 5}$$

The *FVC* was determined in April and September using a grid of 1 m^2 with a mesh width of 0.1 m^2. The visual estimate of each mesh was averaged for the entire square meter. This procedure was repeated four times for each plot. The maximum standard deviation was approx. 5%. For the *Alnus viridis* sites we used the value provided by the US Department of Agriculture (1977) i.e. 0.003. This value assumes a fall height of 0.5 m and a ground cover of 95-100%.

The uncertainty assessment of the RUSLE estimates is based on the measurement error of the plot steepness (± 2%), which was determined by repeated measurements and slope length (± 12.5 m). An error of ± 2% was assumed for the grain size analyses as well as for the organic carbon determination. These errors were propagated through the K-factor calculation. An error of ± 20% based on the observed variability between spring and autumn of FVC on the plots, was used for the determination of the C-factor. For the R-factor an error of ± 5 N h^{-1}, which corresponds to the observed variability between the sites was assumed. Finally error propagation for the multiplication of the single RUSLE factors was done.

2.3.3 ^{137}Cs to assess total net soil redistribution

A 2 x 2 inch NaI-scintillation detector (Sarad, Dresden, Germany) was used to measure the in-situ ^{137}Cs activity. The detector was mounted perpendicular to

259 the ground at a height of 25 cm to reduce the radius of the investigated area to
260 1 meter. Measurement time was set at 3600 seconds and each site was
261 measured three times.
262 The detector was successfully (R^2 = 0.86) calibrated against gamma
263 spectroscopy laboratory measurements with a 20% relative efficiency Li-drifted
264 Ge detector (GeLi; Princeton Gamma-Tech, Princeton, NJ, USA) at the
265 Department for Physics and Astronomy, University of Basel. For the GeLi detector
266 the resulting measurement uncertainty on ^{137}Cs peak area (at 662 keV) was
267 lower than 8% (error of the measurement at 1-sigma) (Schaub et al.,
268 2010).Gamma spectrometry calibration and quality control of the analysis were
269 performed following the protocol proposed by Shakhashiro and Mabit (2009).
270 Soil moisture influences the measured ^{137}Cs activity. Thus, soil moisture
271 measurements with an EC-5 sensor (DecagonDevices) were used to correct the
272 in-situ measurements. The NaI detector has the advantage of providing an
273 integrated measurement over an area of 1 m^2. The commonly observed intrinsic
274 small scale variability (~30 %) for ^{137}Cs (Sutherland, 1996; Kirchner, 2013) is thus,
275 smoothed. Nonetheless, around 10% of the uncertainty of the ^{137}Cs-based soil
276 erosion values can be attributed to the variability of replicated measurements
277 on each single plot. The main error of the in-situ measurement results from the
278 peak area evaluation and was determined at 17 % (Schaub et al., 2010).
279 With the ^{137}Cs method soil redistribution rates are calculated by comparing the
280 isotope inventory for an eroding point with a local reference inventory where
281 neither erosion nor soil accumulation is expected. In the Urseren Valley, the
282 initial reference ^{137}Cs fallout originated from thermonuclear weapon tests in the
283 1950s-1960s and the nuclear power plant accident of Chernobyl in 1986.
284 For the conversion of the ^{137}Cs inventories to soil erosion rates knowledge about
285 the proportion of Chernobyl ^{137}Cs fallout is a key parameter for the estimation of

286 erosion rates, however, only little data is available. Pre-Chernobyl (1986) ^{137}Cs
287 activities of the top soil layers (0 – 5 cm) between 2 and 58 Bq kg^{-1} (one outlier
288 of 188 Bq kg^{-1} in Ticino) were recorded for 12 sites distributed over Switzerland
289 (Riesen et al., 1999). After radioactive decay, in 2007 only 1 – 35 Bq kg^{-1} are left.
290 The ^{137}Cs activity for the flat reference sites near the valley bottom (1469-1616 m
291 a.s.l) was estimated as 146 ± 20 Bq kg^{-1} (Schaub et al., 2010). The investigated
292 sites are located in close vicinity to the reference sites and at comparable
293 altitude (1476-1670 m a.s.l). Consequently, the maximum contribution of pre-
294 Chernobyl ^{137}Cs might represent 20% at reference sites.
295 Additionally, vertical migration must be considered. In literature migration
296 values between 0.03 and 1.30 cm yr^{-1} are reported (Schimmack et al., 1989;
297 Arapis and Karandinos, 2004; Schuller et al., 2004; Schimmack and Schultz, 2006;
298 Ajayi et al., 2007). In the Urseren Valley, ^{137}Cs activity (Bq kg^{-1}) declines
299 exponentially with soil depth. Therefore, for the conversion of ^{137}Cs
300 measurements to soil erosion rates, the well-known profile distribution model
301 (Walling et al., 2011) was adapted for the direct use with ^{137}Cs activity profile
302 (Konz et al., 2009; Konz et al., 2012). We set the particle size factor to 1,
303 because no preferential transport of the finer soil particles was observed for our
304 sites (Konz et al., 2012). In contrast, no preferential transport or preferential
305 transport of coarse material occurred, most likely due to snow and animal
306 induced particle transport (see Konz et al., 2012). The calculation of the erosion
307 rates refers to the period 1986-2007 because pre-Chernobyl ^{137}Cs is negligible.
308 For uncultivated sites the Diffusion and Migration model is an alternative to the
309 profile distribution model. However, the ^{137}Cs depth profile at our reference sites
310 did not follow a polynomial distribution and thus did not allow for a successful fit
311 of the diffusion and migration coefficient. Due to the integrative and repeated
312 measurement with the NaI detector, the errors associated with measurement

313 precision are assumed to be largely cancelled out. However the error
314 associated with the spatial variability of the reference inventory (± 20 Bq kg^{-1})
315 were propagated through the conversion model in order to receive an upper
316 and lower confidence interval for the resulting erosion estimates.

317 *2.4 Spatial modelling of snow glide distances*

318 We used the Spatial Snow Glide Model (SSGM, Leitinger et al. 2008) to predict
319 potential snow glide distances for an area of approximately 30 km^2 surrounding
320 our study sites. The SSGM is an experimental model, which includes the
321 parameters: the forest stand, the slope angle, the winter precipitation, the slope
322 and the static friction coefficient μ_s (-). Slope angle and slope aspect were
323 derived from the digital elevation models DHM25 and below 2000 m a.s.l. the
324 DOM. The DOM is a high precision digital surface model with 2 m resolution and
325 an accuracy of ± 0.5 m at 1σ in open terrain and ± 1.5 m at 1σ in terrain with
326 vegetation. The DHM25 has a resolution of 25 m with an average error of 1.5 m
327 for the Central Plateau and the Jura, 2 m for the Pre-Alps and the Ticino and 3
328 to 8 m for the Alps (Swisstopo). Winter precipitation was derived from the
329 MeteoSwiss station located in Andermatt. We used the result from a QuickBird
330 land cover classification with a resolution of 2.4 m (subsequently resampled to 5
331 m) as land cover input (Meusburger et al., 2010a). Combining this land cover
332 map with a land use map (Meusburger and Alewell, 2009), it was possible to
333 derive the parameter forest stand. To each of the 4 investigated land cover
334 types a uniform static friction coefficient (μ_s) was assigned.
335 The static friction coefficient can be derived by:

336 $$\mu_s = \frac{F_r}{F_n}$$ **Equation 6**

337 where *Fn* (g m s^{-2}) is the normal force that can be calculated with

338 $$F_n = m \times g \times \cos\alpha$$ **Equation 7**

339 where g is the standard gravity (9.81 m s^{-2}), α is the slope angle (°) and m the
340 weight of the snow glide shoe (in our study 202 g).
341 The initial force (*Fr;* with the unit g m s^{-2}), which is needed to get the glide shoe
342 moving on the vegetation surface, was measured with a spring balance (Pesola®
343 Medio 1000 g) and multiplied with the standard gravity. To obtain representative
344 values of *Fr* the measurement was replicated 10 times per sample site and
345 subsequently averaged. The parameter estimates the surface roughness, which
346 integrates the effect of different vegetation types and land uses on snow
347 gliding. A detailed description of the model and its parameters has been
348 provided by Leitinger et al. (2008).
349 Supplemented by snow glide measurements from this study, the SSGM (i.e. OLS
350 regression equation) was refined to be valid also for north exposed sites and
351 sites with *Alnus viridis*. Consequently, the revised SSGM is given by the equation:

352 $$\ln(\hat{y}) = -0.337 - 0.925x_1 + 0.095x_2 + 0.01x_3 + 1.006x_4 + 0.839x_5 + 0.076x_6 - 0.075x_7^2$$ **Equation 8**

353 where $\hat{y}$ is the estimated snow-gliding distance (mm), x_1 is the forest stand (0;1),
354 x_2 is slope angle (°), x_3 is winter precipitation (mm), x_4 is slope aspect East (0;1),
355 x_5 is slope aspect South (0;1), x_6 is slope aspect W (0;1) and x_7 is the static
356 friction coefficient. The revised SSGM was highly significant ($p < 0.001$) with a
357 determination coefficient of 0.581 (adjusted R^2).
358 The model was then applied for the winter period 2009/2010 (285 mm winter
359 precipitation) and for the long-term average winter precipitation (430 mm
360 winter precipitation, years 1959 to 2010).

3 Results and Discussion

3.1 Snow glide measurements 2009/2010

For each site the static friction coefficient as a measure for surface roughness was determined in autumn prior to the installation of the snow glide shoes. Lowest surface roughness was observed for the hayfields, followed by soil surface at sites covered with *Alnus viridis* on the north facing slope (Table 1). For the pastures without dwarf-shrubs, the two mean monitored values differed (μ_s = 0.37 and 0.68) but were similar to that of pastures with dwarf-shrubs (μ_s = 0.66 to 0.69). Slightly higher values were observed for the dense undergrowth of *Alnus viridis* sites on the south facing slope (μ_s = 0.70 and 0.84). These static friction coefficients are within the range of 0.22-1.18 reported by Leitinger et al. (2008). The snow glide measurements confirmed the presence and the potential impact of this process in our investigated sites. The mean measured snow glide distances (sgd) of the different sites varied from 2 to 189 cm (see Table 1). A main proportion of this variability can be explained by the slope aspect and the surface roughness (see Fig. 3). With increasing surface roughness (expressed as the static friction coefficient; μ_s) the snow glide distance declines. This decrease is more pronounced for the south facing slope ($sgd = -1547.2\mu_s + 172.93$; R^2 = 0.50; p = 0.036). For the north facing slope the snow glide distances and the variability are lower. Approximately 80% of the observed variability on the north facing slope can be explained by the surface roughness ($sgd = -622.17\mu_s + 43.09$; R^2 = 0.82; p = 0.033). The identification of slope aspect and surface roughness as main causal factors for snow gliding, corresponds to the findings of other studies (In der Gand and Zupancic, 1966; Newesely et al., 2000; Hoeller et al., 2009). According to several studies on the seasonal snow – soil interface conditions (In der Gand and Zupancic, 1966; McClung and Clarke, 1987; Leitinger et al., 2008),

snow gliding on south-facing sites is preferential in spring, when high solar radiation leads to a high portion of melting water at the soil/snow interface. However, in autumn snow gliding primarily occurs when a huge amount of snow falls on the warm soil. In this case, north-facing sites may be confronted with high snow gliding activity as well.

Our measured snow glide distances are comparable to those recorded by other researchers. For example Höller et al. (2009) monitored during a seven-year period in the Austrian Alps a snow glide distance of 10 cm within the forest, 170 cm in cleared forest sites and up to 320 cm for open fields. Margreth (2007) found total glide distances of 19 to 102 cm for an eleven-year observation period in the Swiss East Alps (south-east facing slope at 1540 m a.s.l.).

3.2 Soil erosion estimates

Snow glide depositions were observed for seven sites, for one site a wet avalanche deposition (pN) and for 4 sites no snow glide depositions were observed (Table 3). The 4 sites without snow glide depositions were all located at the north facing slope. The erosion rates estimated from the sediment yields of the snow glide deposition ranged from 0.03 to 22.9 t ha^{-1} yr^{-1}. The maximum value was determined for the site h1 which is in agreement with the ^{137}Cs method. For sites with snow glide depositions, a mean value of 8.4 t ha^{-1} yr^{-1} was measured. The somewhat high erosion rates are documented in a photo from the spring (Fig. 4). The winter 2012/2013 precipitation of 407 mm was quite representative of the long-term average (i.e. 430 mm). On average, the pastured sites without dwarf shrubs produced the highest measured sediment yields, followed by the hayfields and considerably lower values were observed for the pastures with dwarf shrub sites. Whether the observed difference is due to the different vegetation cover or due to site specific topography cannot be

solved conclusively with the present dataset. A wet avalanche was observed for the site pN. Interestingly, the estimated erosion rate of the wet avalanche deposition was smaller than most of the snow gliding related erosion rates, at 1.97 t ha^{-1} yr^{-1}. However, high erosion rates of 3.7 and 20.8 t ha^{-1} per winter due to wet avalanches have been reported in a study site located in the Aosta Valley, Italy (Ceaglio et al., 2012). In this study site where the major soil loss is triggered by wet avalanches, the snow-related soil erosion estimated from the deposition area was comparable to the yearly total erosion rates assessed with the ^{137}Cs method (13.4 and 8.8 t ha^{-1} yr^{-1}, Ceaglio et al., 2012).

On the north facing slope an average RUSLE estimate of 1.8 t ha^{-1} yr^{-1} with a maximum value of 3.8 t ha^{-1} yr^{-1} was established (Table 2). The on average lower values as compared to the south-facing slope (6.7 t ha^{-1} yr^{-1}) are due to lower slope angles (thus lower LS-factor values) and C-factors (due to a higher fractional vegetation cover). This effect was not compensated by the on average higher K-factor of 0.40 kg h N^{-1} m^{-2} on the north facing slopes. The higher K-factor is caused by a 6 % higher proportion of very fine sand. The mean RUSLE based soil erosion rate for all sites was 4.6 t ha^{-1} yr^{-1}.

The mean ^{137}Cs based soil erosion rates of 17.8 t ha^{-1} yr^{-1} are approximately four times as high as the average RUSLE estimates. Congruent with RUSLE the ^{137}Cs-based average soil erosion rate on the north facing slopes is lower than on the south facing slopes (by 8.7 t ha^{-1} yr^{-1}). The highest ^{137}Cs-based soil erosion estimates are found at two hayfield sites (h1 and h3) and the pasture sites at the south facing slope (p1 and p2). The higher RUSLE and ^{137}Cs estimates on the more intensely used, steeper and more snow glide affected south facing slope are reasonable. However, the high ^{137}Cs-based erosion rates (16.6 t ha^{-1} yr^{-1} for A1N and 13.7 t ha^{-1} yr^{-1} for A2N)) at *Alnus viridis* sites are unexpected and will be discussed below.

3.3 Relation between soil redistribution and snow gliding

Sediment yield measurements in snow glide depositions showed the importance of this process in the winter 2012/2013. However, even though the winter was quite representative for the average winter conditions (in terms of winter precipitation) the measured rates are likely to vary between different years. To assess the relevance of this process for a longer time scale, a second approach using RUSLE and ^{137}Cs was followed.

Our hypothesis was that the difference of the water soil erosion rate modelled with RUSLE and the total net erosion measured with the ^{137}Cs method correlates to a "winter soil erosion rate". This winter soil erosion rate comprises long-term soil removal by snow gliding and occasionally wet avalanches as well as snow melt. These "winter erosion rates" (difference of ^{137}Cs and RUSLE) ranged from ~~sedimentation~~ rates of -7~~3~~.3 t ha^{-1} yr^{-1} for a pasture with dwarf shrubs to ~~erosion~~ rates of 31 t ha^{-1} yr^{-1} for the hayfield site h1. A negative difference of ^{137}Cs and RUSLE indicates, according to our hypothesis, a sedimentation (because RUSLE simulates the potential water soil erosion rates) and a positive value erosion due to processes not implemented in the RUSLE. The most likely processes would be snow induced processes. Two observations underpin our hypothesis:

first, even though the sediment yield measurements in the snow glide deposition comprise only one winter, a relation ($p = 0.13$) between the snow glide erosion and the difference of ^{137}Cs and RUSLE could be observed ($R^2 = 0.39$; Fig. 5~~4~~). The largest~~highest~~ difference between ^{137}Cs and RUSLE based erosion could be observed for sites with high snow glide related sediment yield (except for the site h3). The resulting intercept might be either to a deviation of the weather conditions in the winter 2012/2013 from the long-term average condition captured by the other methods or due to the impact of occasional wet

avalanches and/or snow melt. For instance, following the USLE snow melt adaptation for R-factor would result in an on average 2.1 t ha^{-1} yr^{-1} higher modelled erosion rate for all sites.

A further indication for the importance of snow gliding as soil erosion agent is given by the significant positive correlation between measured snow glide distance and the difference of ^{137}Cs and RUSLE, which we interpret as winter soil erosion rate (Fig. 6~~5~~). The measured snow glide distance explained 64 % of the variability of the winter soil erosion rate ($p<0.005$). However, this relation does not comprise the *Alnus viridis* sites that showed a large~~high~~ difference between RUSLE and ^{137}Cs based rates but a low snow glide distance. For the *Alnus viridis* sites, we have to expect that either one of the two approaches to determine soil erosion rates is erroneous and/or that we have another predominant erosion process not considered/or not correctly parameterised in the RUSLE yet. A possible error related to the ^{137}Cs approach might be that ^{137}Cs was intercepted by leaf and litter material of *Alnus viridis*. Thus, a reference site with *Alnus viridis* stocking would be necessary which is difficult to find in our site because no flat areas exist with *Alnus viridis* stocking. The observation of increasing soil erosion with increasing snow glide rates is congruent with the findings of Leitinger et al. (2008), who observed that the severity of erosion attributed to snow gliding (e.g. torn out trees, extensive areas of bare soil due to snow abrasion, landslides in topsoil) was high in areas with high snow glide distance and vice versa.

Generally, for these sub-alpine sites the magnitude of the RUSLE based water erosion rates need to be considered with caution not only with respect to the involved uncertainties but also conceptually since several of the factors lay outside the empirical RUSLE framework. Also the magnitude of the ^{137}Cs based erosion rate needs to be considered carefully. The profile distribution model tends to overestimate soil erosion rates since it assumes that the ^{137}Cs depth

distribution does not change with time. However, in the very first years after the fallout, ^{137}Cs was concentrated more in the surface soil layer (Schimmack and Schultz, 2006). Thus, in the years after the fallout small losses of soil would have resulted in a relatively high ^{137}Cs loss which might result in an overestimation of soil erosion rates.

The latter uncertainties do not include snow melt erosion and temporal variability, both potential reasons for the intercept observed between the magnitude of winter erosion estimated from RUSLE/^{137}Cs and from snow glide depositions. Nonetheless, the almost 1:1 relation is a clear indication that the observed discrepancies between the RUSLE and ^{137}Cs based soil erosion rates are related to snow gliding. Congruent with our results Stanchi et al. (2014, accepted) found a relation between the intensity of snow erosion affected areas and the difference of RUSLE and ^{137}Cs estimates.

Further, it can be deduced that low surface roughness is correlated to high snow glide distances and these are again positively correlated to large~~high~~ observed differences between RUSLE and ^{137}Cs based soil erosion rates that we interpret as high winter soil erosion rates. Erosion estimates from sediment yield measurements of the snow glide deposition could confirm the partially high winter erosion rates. However, the presented relations might be highly variable, depending on soil temperature (whether the soil is frozen or not) during snow in, the occurrence of a water film that allows a transition of dry to wet gliding (Haefeli, 1948) and on the weather conditions of a specific winter. In addition, some of the investigated sites might also be affected by avalanches in other years.

3.4 Modelled snow glide distances

The modelled snow glide rates from the SSGM compared reasonably well with the snow glide measurements (Fig. 7~~6~~). In agreement with the measured values all sites facing to the north revealed lower modelled snow glide distances. Largest discrepancies between the mean modelled and measured values of each site occur for the pastures on the south facing slopes (p and pw). The model overestimates the snow glide rates for these sites, which might be due to the effect of micro-relief in form of cattle trails at these sites. This small terraces (0.5 m in width) most likely reduce snow gliding but are not captured by the digital elevation model that is used for the SSGM. In general, modelled snow glide distances show smaller ranges than measured snow glide distances, due to the 5 m resolution of the model input data (Fig. 7~~6~~). Interestingly, the occurrence of dwarf shrubs seems to reduce snow gliding to a larger extend as predicted by the model.

The modelled snow glide distance map (Fig. 8~~7~~) is based on the long-term average of winter precipitation, which is with 430 mm clearly higher than the winter precipitation in 2009/2010 with 285 mm (Fig. 7~~6~~). The highest snow glide values were simulated on the steep, south facing slopes with predominate grassland and dwarf-shrub cover. Very high rates are also found on the lower parts of the south facing slopes that are used as pastures and hayfields. The smallest snow glide rates are located on the north facing slopes. The map clearly reproduces the effect of topography and aspect. Moreover, snow glide distances summarized for predominant land-use types also reproduce the impact of vegetation cover (Fig. 9~~8~~). The highest potential snow glide distances were simulated by the SSGM for the south-facing hayfield and pasture sites while the *Alnus viridis* has on average decisively smaller snow glide distances. In

contrast, on the north facing slopes there is no difference observed between the *Alnus viridis* - and the hayfield category. Here the pasture sites show the highest average snow glide rate. The interpretation of the differences between land use types is, however, restricted since systematically different topographic conditions are involved.

The topographic and climatic conditions in our valley resemble the environment under which the SSGM was initially developed; nonetheless further regular yearly measurement would be needed to improve the performance of the model in this area. In conclusion, the application of the SSGM highlighted the relevance of the snow gliding process and the potentially related soil erosion for (sub-) alpine areas.

4 Conclusions

The presented absolute magnitude of the snow glide related soil erosion rate is subject to high ~~uncertainties and~~ inter-annual variability. However, snow glide erosion ~~estimated~~ measured from the snow glide deposition<u>s</u> (0.03 to 22.9 t ha^{-1} yr^{-1} in the winter 2012/2013) <u>highlights the need to consider the process of snow gliding as a soil erosion agent in steep, scarcely vegetated alpine areas.</u>

<u>RUSLE and ^{137}Cs both yield average long-term soil erosion rates for water and total net erosion, respectively. Despite the associated uncertainties, the total net erosion rate is significantly higher than the gross water erosion rate provided by RUSLE. We interpret the difference as "winter" soil erosion rate which was significantly correlated to snow glide rates and showed an almost 1:1 relation to sediment yield measurements in snow glide</u> deposition<u>s. The application of RUSLE and ^{137}Cs showed i) the relevance of the snow glide process for a longer time scale (as compared to the snow glide</u> deposition <u>measurements of one winter)</u>

and ii) that for an accurate soil erosion prediction in high mountain areas it is crucial to assess and quantify the erosivity of snow movements.

The Spatial Snow Glide Model might serve as a tool to evaluate the spatial relevance of snow gliding for larger areas. However, it would be recommended to additionally estimate the kinetic energy that acts upon the soil during the snow movement. This would allow for a direct comparison of rainfall erosivity and snow movement erosivity, and moreover its insertion into soil erosion risk models. The impact of snow movement on soil removal should moreover, be evaluated in context of predicted changes in snow cover e.g. an increase of snow amount for elevated (>2000 m a.s.l.) areas (Beniston, 2006).

Further, we demonstrated that surface roughness, which is determined by the vegetation type and the land use, reduces snow glide rates particularly on the in general more intensely used south facing slopes. In turn snow glide rates are positively related to increasing soil loss for grassland sites. This is an important result with respect to soil conservation strategy since surface roughness can be modified and adapted through an effective land use management.

Acknowledgement

This study was funded by the Swiss Federal Office for the Environment (Contract-no.: StoBoBio/810.3129.004/05/0X).

589

590 References

591

592 Ackroyd, P.: Erosion by snow avalanche and implications for geomorphic
593 stability, Torlesse Range, New-Zealand, Arct. Alp. Res., 19, 65-70,
594 10.2307/1551001, 1987.

595 Ajayi, I. R., Fischer, H. W., Burak, A., Qwasmeh, A., and Tabot, B.: Concentration
596 and vertical distribution of Cs-137 in the undisturbed soil of southwestern
597 Nigeria, Health Phys., 92, 73-77, 2007.

598 Alewell, C., Meusburger, K., Juretzko, G., Mabit, L., and Ketterer, M.: Suitability of
599 $^{239+240}$Pu as a tracer for soil erosion in alpine grasslands, Chemosphere, 103, 274-
600 280, doi: 10.1016/j.chemosphere.2013.12.016., 2014.

601 Arapis, G. D., and Karandinos, M. G.: Migration of Cs-137 in the soil of sloping
602 semi-natural ecosystems in Northern Greece, Journal of Environmental
603 Radioactivity, 77, 133-142, 10.1016/j.jenvrad.2004.03.004, 2004.

604 Bell, I., Gardner, J., and Descally, F.: An estimate of snow avalanche debris
605 transport, Kaghan Valley, Himalaya, Pakistan, Arct. Alp. Res., 22, 317-321,
606 10.2307/1551594, 1990.

607 Beniston, M.: Mountain weather and climate: A general overview and a focus on
608 climatic change in the Alps, Hydrobiologica, 562, 3-16, 2006.

609 Benmansour, M., Mabit, L., Nouira, A., Moussadek, R., Bouksirate, H., Duchemin,
610 M., and Benkdad, A.: Assessment of soil erosion and deposition rates in a
611 Moroccan agricultural field using fallout 137Cs and 210Pbex, Journal of
612 Environmental Radioactivity, 115, 97-106, 10.1016/j.jenvrad.2012.07.013, 2013.

613 Ceaglio, E., Meusburger, K., Freppaz, M., Zanini, E., and Alewell, C.: Estimation of
614 soil redistribution rates due to snow cover related processes in a mountainous
615 area (Valle d'Aosta, NW Italy), Hydrology and Earth System Sciences, 16, 517–
616 528, 2012.

617 Confortola, G., Maggioni, M., Freppaz, M., and Bocchiola, D.: Modelling soil
618 removal from snow avalanches: A case study in the North-Western Italian Alps,
619 Cold Regions Science and Technology, 70, 43-52,
620 10.1016/j.coldregions.2011.09.008, 2012.

621 Foster, G. R., and Highfill, R. E.: Effect of terraces on soil loss - USLE P-factor
622 values for terraces, Journal Of Soil And Water Conservation, 38, 48-51, 1983.

623 Freppaz, M., Godone, D., Filippa, G., Maggioni, M., Lunardi, S., Williams, M. W.,
624 and Zanini, E.: Soil Erosion Caused by Snow Avalanches: a Case Study in the
625 Aosta Valley (NW Italy), Arct. Antarct. Alp. Res., 42, 412-421, 10.1657/1938-4246-
626 42.4.412, 2010.

627 Fuchs, S., and Keiler, M.: Variability of Natural Hazard Risk in the European Alps:
628 Evidence from Damage Potential Exposed to Snow Avalanches, Disaster
629 Mangement Handbook, edited by: Pinkowski, J., Crc Press-Taylor & Francis
630 Group, Boca Raton, 267-279 pp., 2008.

631 Gardner, J. S.: Observations on erosion by wet snow avalanches, Mount Rae
632 area, Alberta, Canada, Arct. Alp. Res., 15, 271-274, 10.2307/1550929, 1983.

633 Haefeli, R.: Schnee, Lawinen, Firn und Gletscher, Ingenieur-Geologie, edited by:
634 Bendel, L., Springer Vienna, Wien, 1948.

635 Heckmann, T., Wichmann, V., and Becht, M.: Sediment transport by avalanches
636 in the Bavarian Alps revisited - a perspective on modelling, in: Geomorphology
637 in Environmental Application:, edited by: Schmidt, K. H., Becht, M., Brunotte, E.,
638 Eitel, B., and Schrott, L., Zeitschrift Fur Geomorphologie Supplement Series,
639 Gebruder Borntraeger, Stuttgart, 11-25, 2005.

640 Hoeller, P., Fromm, R., and Leitinger, G.: Snow forces on forest plants due to
641 creep and glide, Forest Ecology and Management, 257, 546-552,
642 10.1016/j.foreco.2008.09.035, 2009.

643 Holler, P., Fromm, R., and Leitinger, G.: Snow forces on forest plants due to
644 creep and glide, Forest Ecology and Management, 257, 546-552,
645 10.1016/j.foreco.2008.09.035, 2009.

In der Gand, H. R., and Zupancic, M.: Snow gliding and avalanches, IAHS-AISH Publ, 69, 230-242, 1966.

Jomelli, V., and Bertran, P.: Wet snow avalanche deposits in the French Alps: Structure and sedimentology, Geogr. Ann. Ser. A-Phys. Geogr., 83A, 15-28, 10.1111/j.0435-3676.2001.00141.x, 2001.

Juretzko, G.: Quantifizierung der Bodenerosion mit 137Cs und USLE in einem alpinen Hochtal (Val Piora, CH), Master, Environmental Sciences, Basel, Basel, 1-152 pp., 2010.

Kinnell, P. I. A.: Why the universal soil loss equation and the revised version of it do not predict event erosion well, Hydrological Processes, 19, 851-854, 10.1002/hyp.5816, 2005.

Kinnell, P. I. A.: Event soil loss, runoff and the Universal Soil Loss Equation family of models: A review, Journal of Hydrology, 385, 384-397, 10.1016/j.jhydrol.2010.01.024, 2010.

Kirchner, G.: Establishing reference inventories of Cs-137 for soil erosion studies: Methodological aspects, Geoderma, 211, 107-115, 10.1016/j.geoderma.2013.07.011, 2013.

Konz, N., Schaub, M., Prasuhn, V., Bänninger, D., and Alewell, C.: Cesium-137-based erosion-rate determination of a steep mountainous region, Journal of Plant Nutrition and Soil Science, 172, 615-622, 10.1002/jpln.200800297, 2009.

Konz, N., Baenninger, D., Konz, M., Nearing, M., and Alewell, C.: Process identification of soil erosion in steep mountain regions, Hydrology and Earth System Sciences, 14, 675-686, 2010.

Konz, N., Prasuhn, V., and Alewell, C.: On the measurement of alpine soil erosion, CATENA, 91, 63-71, 10.1016/j.catena.2011.09.010, 2012.

Leitinger, G., Holler, P., Tasser, E., Walde, J., and Tappeiner, U.: Development and validation of a spatial snow-glide model, Ecological modelling, 211, 363-374, 10.1016/j.ecolmodel.2007.09.015, 2008.

Mabit, L., Bernard, C., Laverdiere, M. R., Wicherek, S., Garnier, J., and Mouchel, J. M.: Assessment of soil erosion in a small agricultural basin of the St. Lawrence River watershed, Hydrobiologia, 410, 263-268, 1999.

Mabit, L., Bernard, C., and Laverdiere, M. R.: Quantification of soil redistribution and sediment budget in a Canadian watershed from fallout caesium-137 (Cs-137) data, Canadian Journal of Soil Science, 82, 423-431, 2002.

Mabit, L., and Bernard, C.: Assessment of spatial distribution of fallout radionuclides through geostatistics concept, Journal of Environmental Radioactivity, 97, 206-219, 10.1016/j.jenvrad.2007.05.008, 2007.

Mabit, L., Benmansour, M., and Walling, D. E.: Comparative advantages and limitations of the fallout radionuclides Cs-137, Pb-210(ex) and Be-7 for assessing soil erosion and sedimentation, Journal of Environmental Radioactivity, 99, 1799-1807, 10.1016/j.jenvrad.2008.08.009, 2008.

Mabit, L., Meusburger, K., Fulajtar, E., and Alewell, C.: The usefulness of 137Cs as a tracer for soil erosion assessment: A critical reply to Parsons and Foster (2011), Earth-Science Reviews, 137, 300-307, http://dx.doi.org/10.1016/j.earscirev.2013.05.008, 2013.

Margreth, S.: Snow pressure on cableway masts: Analysis of damages and design approach, Cold Regions Science and Technology, 47, 4-15, 10.1016/j.coldregions.2006.08.020, 2007.

Matisoff, G., and Whiting, P. J.: Measuring Soil Erosion Rates Using Natural (Be-7, Pb-210) and Anthropogenic (Cs-137, Pu-239,Pu-240) Radionuclides, Handbook of Environmental Isotope Geochemistry, Vols 1 and 2, edited by: Baskaran, M., Springer-Verlag Berlin, Berlin, 487-519 pp., 2011.

McClung, D. M., and Clarke, G. K. C.: The effects of free-water on snow gliding, Journal of Geophysical Research-Solid Earth and Planets, 92, 6301-6309, 1987.

Merritt, W. S., Letcher, R. A., and Jakeman, A. J.: A review of erosion and sediment transport models, Environmental Modelling & Software, 18, 761-799, 2003.

703 Meusburger, K., and Alewell, C.: On the influence of temporal change on the
704 validity of landslide susceptibility maps, Nat Hazard Earth Sys, 9, 1495-1507, 2009.

705 Meusburger, K., Banninger, D., and Alewell, C.: Estimating vegetation parameter
706 for soil erosion assessment in an alpine catchment by means of QuickBird
707 imagery, International Journal of Applied Earth Observation and
708 Geoinformation, 12, 201-207, 10.1016/j.jag.2010.02.009, 2010a.

709 Meusburger, K., Konz, N., Schaub, M., and Alewell, C.: Soil erosion modelled with
710 USLE and PESERA using QuickBird derived vegetation parameters in an alpine
711 catchment, International Journal of Applied Earth Observation and
712 Geoinformation, 12, 208-215, 10.1016/j.jag.2010.02.004, 2010b.

713 Meusburger, K., Mabit, L., Park, J. H., Sandor, T., and Alewell, C.: Combined use
714 of stable isotopes and fallout radionuclides as soil erosion indicators in a
715 forested mountain site, South Korea, Biogeosciences Discuss., 10, 2565-2589,
716 doi:10.5194/bgd-10-2565-2013, 2013.

717 Nearing, M., Foster, G., Lane, L., and Finkner, S.: A process-based soil erosion
718 model for USDA - water erosion prediction project technology, Transactions of
719 the American Society of Agricultural Engineers, 32, 1587-1593, 1989.

720 Newesely, C., Tasser, E., Spadinger, P., and Cernusca, A.: Effects of land-use
721 changes on snow gliding processes in alpine ecosystems, Basic and Applied
722 Ecology, 1, 61-67, 10.1078/1439-1791-00009, 2000.

723 Panagos, P., Meusburger, K., Van Liedekerke, M., Alewell, C., Hiederer, R., and
724 Montanarella, L.: Assessing soil erosion in Europe based on data collected
725 through a European Network, Soil Science and Plant Nutrition, 1-15,
726 http://dx.doi.org/10.1080/00380768.2013.835701, 2014.

727 Parker, S. P.: McGraw-Hill Dictionary of Scientific and Technical Terms, published
728 by The McGraw-Hill Companies, Inc., New York City, 2002.

729 Renard, K. G., Foster, G. R., Weesies, G. A., MCCool, D. K., and Yoder, D. C.:
730 Predicting soil erosion by water; a guide to conservation planning with the
731 revised universal soil loss equation (RUSLE), US Department of Agriculture, 404,
732 1997.

733 Riesen, T., Zimmermann, S., and Blaser, P.: Spatial Distribution of 137CS in Forest
734 SOils of Switzerland, Water, Air, & Soil Pollution, 114, 277-285,
735 10.1023/a:1005045905690, 1999.

736 Risse, L. M., Nearing, M. A., Nicks, A. D., and Laflen, J. M.: Error assessment in the
737 Universal Soil Loss Equation, Soil Science Society of America Journal, 57, 825-833,
738 1993.

739 Rogler, H., and Schwertmann, U.: Rainfall erosivity and isoerodent map of
740 Bavaria, Zeitschrift für Kulturtechnik und Flurbereinigung, 22, 99-112, 1981.

741 Schaub, M., Konz, N., Meusburger, K., and Alewell, C.: Application of in-situ
742 measurement to determine 137Cs in the Swiss Alps, Journal of Environmental
743 Radioactivity, 101, 369-376, 2010.

744 Schimmack, W., Bunzl, K., and Zelles, L.: Initial rates of migration of radionuclides
745 from the Chernobyl fallout in undisturbed soils, Geoderma, 44, 211-218, 1989.

746 Schimmack, W., and Schultz, W.: Migration of fallout radiocaesium in a grassland
747 soil from 1986 to 2001 - Part 1: Activity-depth profiles of Cs-134 and Cs-137,
748 Science of the Total Environment, 368, 853-862, 2006.

749 Schuller, P., Bunzl, K., Voigt, G., Ellies, A., and Castillo, A.: Global fallout Cs-137
750 accumulation and vertical migration in selected soils from South Patagonia,
751 Journal of Environmental Radioactivity, 71, 43-60, 10.1016/s0265-931x(03)00140-1,
752 2004.

753 Schüpp, M.: Objective weather forecasts using statistical aids in Alps, Rivista
754 Italiana Di Geofisica E Scienze Affini, 1, 32-36, 1975.

755 Smith, S. J., Williams, J. R., Menzel, R. G., and Coleman, G. A.: Prediction of
756 sediment yield from Southern Plains grasslands with the Modified Universal Soil
757 Loss Equation, J. Range Manage., 37, 295-297, 10.2307/3898697, 1984.

758 Stanchi, S., Freppaz, M., Ceaglio, E., Maggioni, M., Meusburger, K., Alewell, C.,
759 and Zanini, E.: Soil erosion in an avalanche release site (Valle d'Aosta: Italy):
760 towards a winter factor for RUSLE in the Alps, NHESSD, 2, 1405-1431,
761 doi:10.5194/nhessd-2-1405-2014, 2014, accepted.

762 Sutherland, R. A.: Caesium-137 soil sampling and inventory variability in
763 reference locations: A literature survey, Hydrological Processes, 10, 43-53, 1996.

764 US Department of Agriculture, S. C. S.: Procedure for computing sheet and rill
765 erosion on project areas, Soil Conservation Service, Technical Release No. 51
766 (Rev. 2), 1977.

767 Walling, D. E., Zhang, Y., and He, Q.: Models for deriving estimates of erosion
768 and deposition rates from fallout radionuclide (caesium-137, excess lead-210,
769 and beryllium-7) measurements and the development of user friendly software
770 for model implementation, in: Impact of Soil Conservation Measures on Erosion
771 Control and Soil Quality, 11–33, 2011.

772 Wischmeier, W. H., and Smith, D. D.: Predicting rainfall-erosion losses from
773 cropland east of the Rocky Mountains, Agriculture Handbook 282, US
774 Department of Agriculture, Washington DC, 1965.

775 Wischmeier, W. H., and Smith, D. D.: Predicting Rainfall Erosion Losses - A Guide
776 to Conservation Planning, USDA/Science and Education Administration, US.
777 Govt. Printing Office, Washington D.C., 58 pp., 1978.
778
779
780

5 Tables

Table 1: Parameters related to measured snow glide distance (sgd, SD = standard deviation based on 3-5 replicate measurements) for the investigation sites in the Ursern Valley, Switzerland. N indicates the sites on the north facing slope.

site	vegetation	slope (°)	initial force Fr (g m s^{-2})	static friction coefficient μs (-)	measured sgd (cm)	SD sgd (cm)
h1	hayfield	39	569	0.37	189	117
h2	hayfield	38	510	0.33	50	40
h3	hayfield	35	392	0.24	126	49
pw1	pasture with dwarf-shrubs	38	1030	0.66	34	19
pw2	pasture with dwarf-shrubs	35	1118	0.69	28	15
p1	pasture	38	579	0.37	89	37
p2	pasture	35	1109	0.68	64	40
h1N	hayfield	28	343	0.20	30	14
h2N	hayfield	30	608	0.35	8	1
pN	pasture	18	628	0.33	17	23
A1N	*Alnus viridis*	25	1050	0.58	2	1
A2N	*Alnus viridis*	30	451	0.26	28	9
A1	*Alnus viridis*	22	1550	0.84	14	18
A2	*Alnus viridis*	31	1197	0.70	60	46

788

789 Table 2: Measured site characteristics (SOC=soil organic carbon; vfs= very fine sand fraction), resulting RUSLE factors

790 and soil erosion rates and ^{137}Cs based erosion rates for the investigation sites in the Ursern Valley, Switzerland.

791 *indicated the sites from Konz et al. (2009).

site	slope (°)	SOC (%)	vfs (%)	silt (%)	clay (%)	K-factor (kg h N^{-1} m^{-2})	P-factor (-)	LS-factor (-)	R-factor (N h^{-1})	C-factor (-)	RUSLE (t ha^{-1} yr^{-1})	^{137}Cs (t ha^{-1} yr^{-1})
h1	39	7.7	12.9	47.3	12.5	0.280	1.00	22.2	97.2	0.010	6.0	37.0
h2	38	7.2	9.7	58.8	17.3	0.290	1.00	8.8	94.5	0.006	1.5	11.0
h3	35	7.4	12.3	43.8	16.9	0.230	1.00	20.7	93.6	0.010	4.5	33.0
pw1	38	6.9	6.3	63.5	10.8	0.320	0.90	12.6	91.7	0.040	13.3	6.0
pw2	35	7.1	11.2	40.9	14.2	0.230	0.90	11.8	94.8	0.040	9.3	13.0
p1	38	7.6	11.2	50.5	11.6	0.270	0.90	11.8	97.6	0.020	5.6	20.0
p2	35	7.2	12.4	45.6	15.0	0.250	0.90	15.3	96.4	0.020	6.6	30.0
h1N	28	4.8	18.5	41.0	5.8	0.416	1.00	7.0	93.6	0.012	3.2	18.3
h2N	30	4.3	13.7	48.0	8.5	0.419	1.00	8.4	91.7	0.012	3.8	7.5
pN	18	6.2	17.5	38.7	10.2	0.369	1.00	1.1	97.2	0.012	0.5	7.2
A1N	25	3.8	16.1	43.8	9.7	0.399	1.00	5.3	93.6	0.003	0.6	16.6
A2N	30	6.8	18.7	39.7	9.6	0.389	1.00	8.4	91.7	0.003	0.9	13.7
Mean of N-facing sites	37	7.3	10.9	50.1	14.0	0.267	0.94	14.7	95.1	0.021	6.7	21.4
Mean of S-facing sites	26	5.2	16.9	42.2	8.8	0.398	1.00	6.0	93.6	0.008	1.8	12.7
mean of all sites	32.4	6.4	13.4	46.8	11.8	0.3	1.0	11.1	94.5	0.0	4.6	17.8

792

793

Table 3: Snow movement related soil erosion derived from the difference of ^{137}Cs-based and RUSLE-based erosion rates (Diff.) and from field measured sediment in snow glide deposits (sg erosion). For each snow glide deposit, the mean sediment yield estimate is based on several samples (n). SD = is the standard deviation for the resulting erosion rates based on the individual sediment yield samples and * indicates the sediment yield of a wet avalanche. Uncertainty Diff. provides the uncertainty of Diff. resulting from both the ^{137}Cs and RUSLE method.

site	RUSLE (t ha^{-1} yr^{-1})	^{137}Cs (t ha^{-1} yr^{-1})	Diff. ^{137}Cs - RUSLE (t ha^{-1} yr^{-1})	Uncertainty Diff. (t ha^{-1} yr^{-1})	sg erosion (t ha^{-1} yr^{-1})	SD sg erosion (t ha^{-1} yr^{-1})	n
h1	6.0	37.0	31.0	8.5	22.9	81.5	16
h2	1.5	11.0	9.5	7.7	3.2	1.9	3
h3	4.5	33.0	28.5	8.2	1.1	1.9	10
pw1	13.3	6.0	-7.3	10.9	0.8	0.5	3
pw2	9.3	13.0	3.7	9.8	0.0	0.1	7
p1	5.6	20.0	14.4	8.5	16.7	6.8	11
p2	6.6	30.0	23.4	8.6	14.0	44.9	13
h1N	3.2	18.3	15.1	7.6	no snow glide	-	-
h2N	3.8	7.5	3.7	8.4	no snow glide	-	-
pN	0.5	7.2	6.7	8.0	1.97*	3.8	18
A1N	0.6	16.6	16.0	7.2	no snow glide	-	-
A2N	0.9	13.7	12.8	7.6	no snow glide	-	-

6 Figure captions

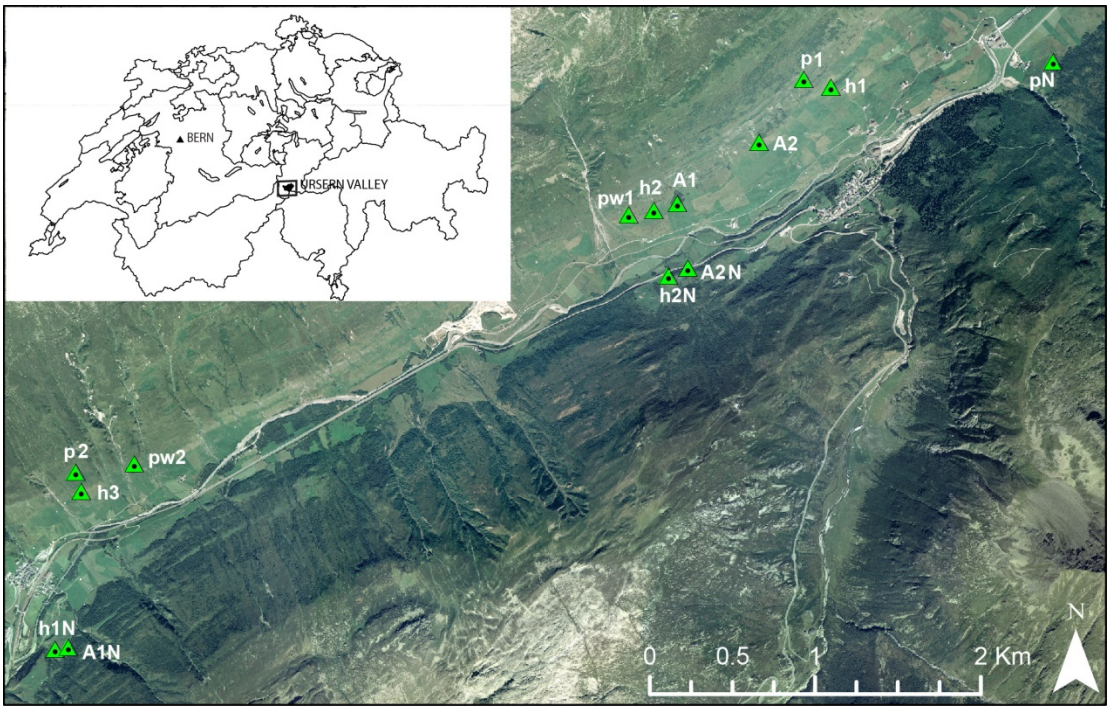

Fig. 1 The Ursern Valley in the Central Swiss Alps and the location of the 14 investigated sites (hayfields (h), pastures (p), pastures with dwarf shrubs (pw), and abandoned grassland covered with *Alnus viridis* (A), north facing slope (N)).

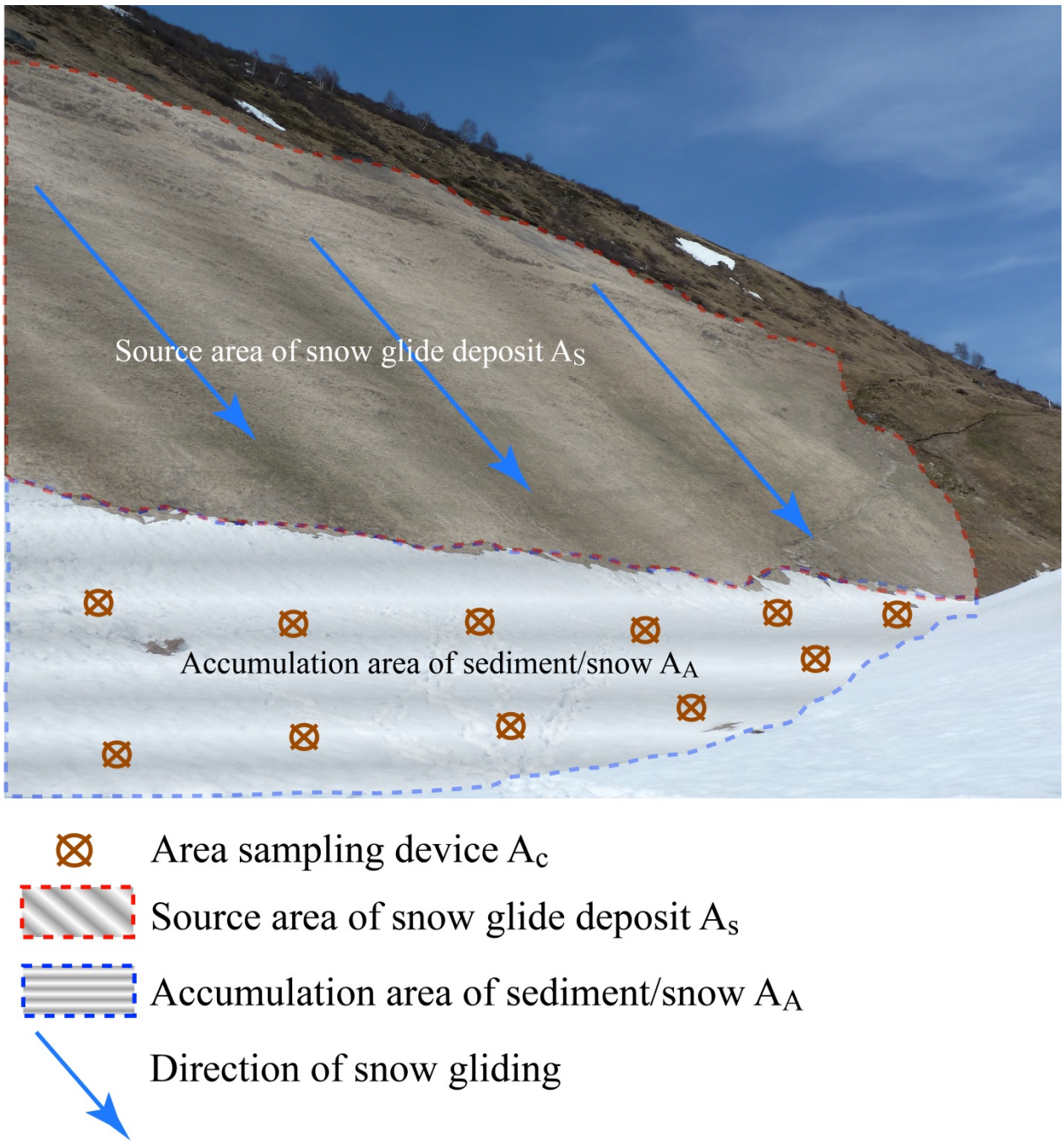

807

808 Fig.2 Illustration of the procedure for snow glide related erosion rate assessment.

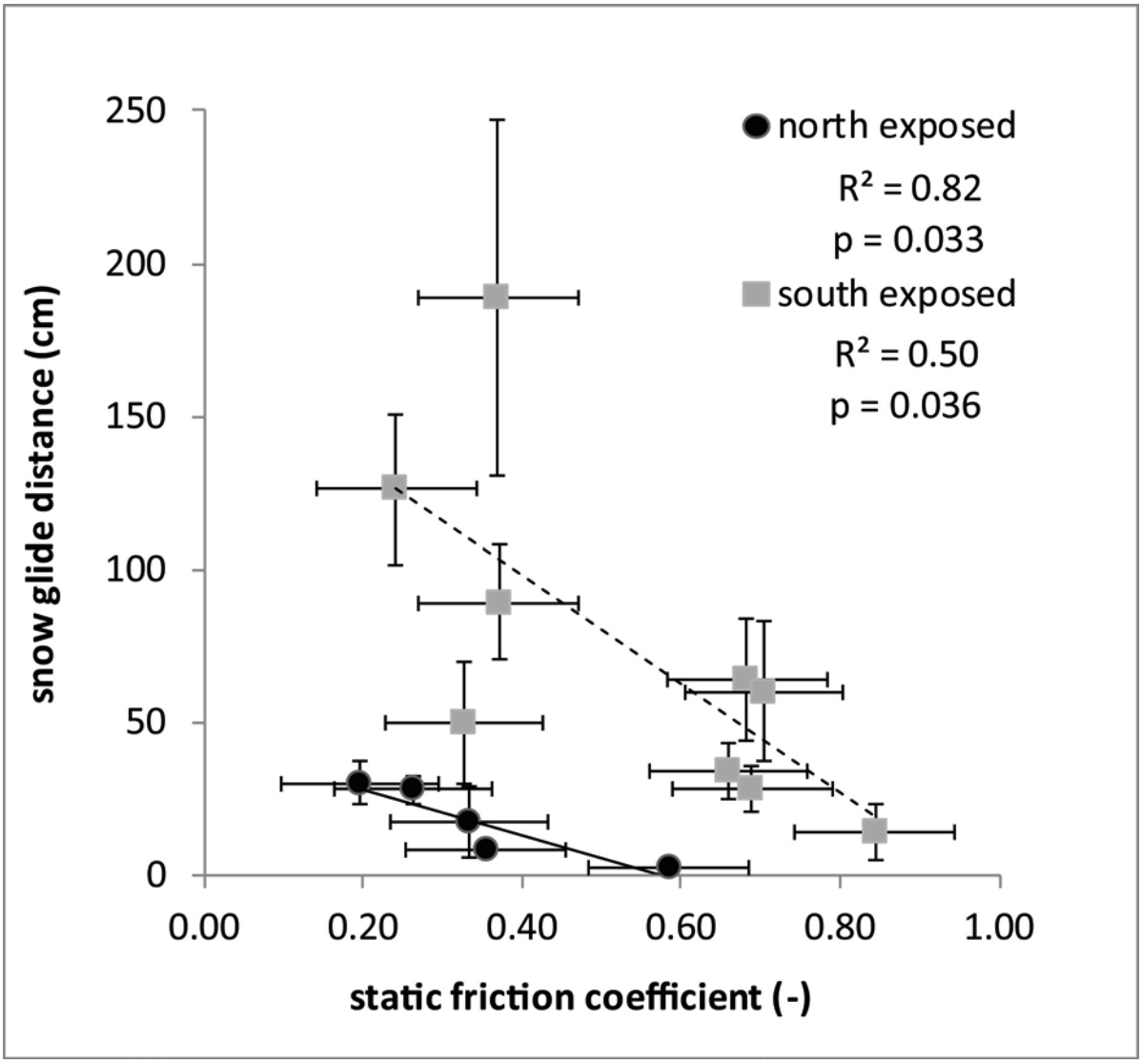

Fig. 3 Snow glide distance against the static friction coefficient for the south- (squares) and north (dots) facing slope sites. Y-error bars represent the standard deviation of replicate measurements at one site. For the static friction coefficient, an error of ± 0.1 (corresponding to the scale accuracy of the spring balance) was assumed.

Fig. 4 Example of snow glide deposits for the site p1.

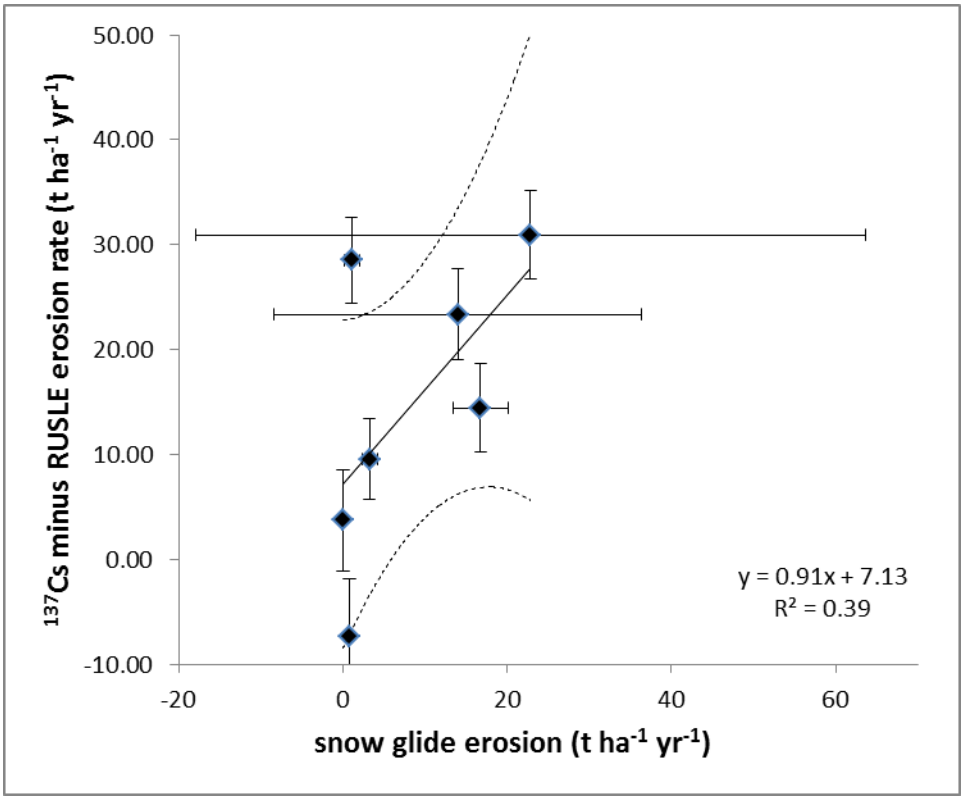

Fig. 54 ~~4~~ Snow glide erosion estimated from the snow glide deposit sediment yield against the difference of the ^{137}Cs and RUSLE soil erosion rate (t ha^{-1} yr^{-1}).Y-error bars represent the uncertainty of both the ^{137}Cs and RUSLE estimates. X-error bars represent the standard deviation of erosion rates resulting from several sediment ~~several~~ measurements within one snow glide deposit. The solid line represents the obtained linear regression and the dotted lines the 95% confidence interval.

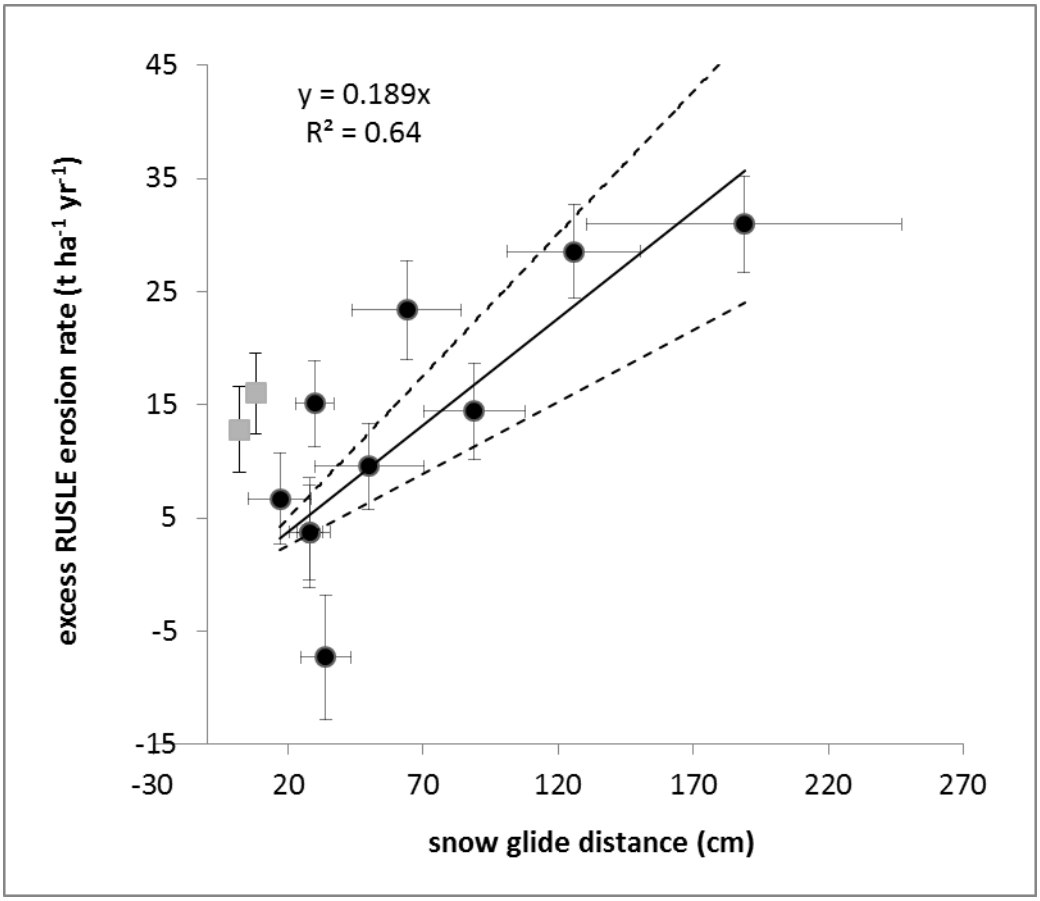

Fig. 6~~5~~ Correlation of the cumulative snow glide distances (cm) measured for the winter 2009/2010 versus the difference of the ^{137}Cs and RUSLE soil erosion rate (t ha^{-1} yr^{-1}) for the grassland sites (dots, n=10) and the *Alnus viridis* sites A1N, A2N (squares, n=2). Y-error bars represent the error of both the ^{137}Cs and RUSLE estimates. X-error bars represent the standard deviation of replicate snow glide measurements at one site. Solid line represents a linear regression and the dotted lines the 95% confidence interval.

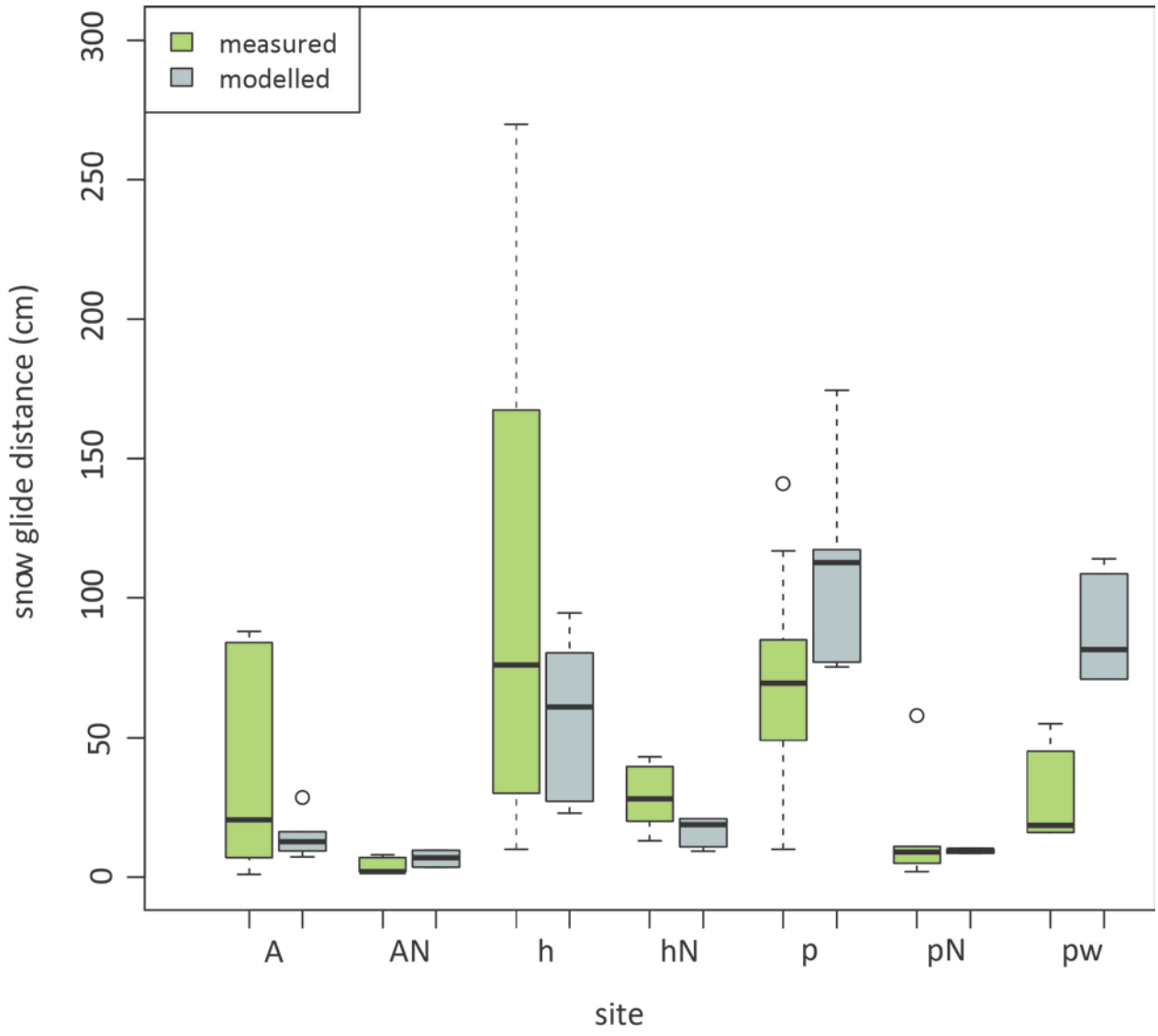

Fig. 7~~6~~ Boxplot of measured snow glide distances and corresponding modelling results for different land use/cover types (hayfields (h), pastures (p), pastures with dwarf shrubs (pw), and abandoned grassland covered with *Alnus viridis* (A)) for the winter period 2009/2010. N indicates the sites on the north facing slope.

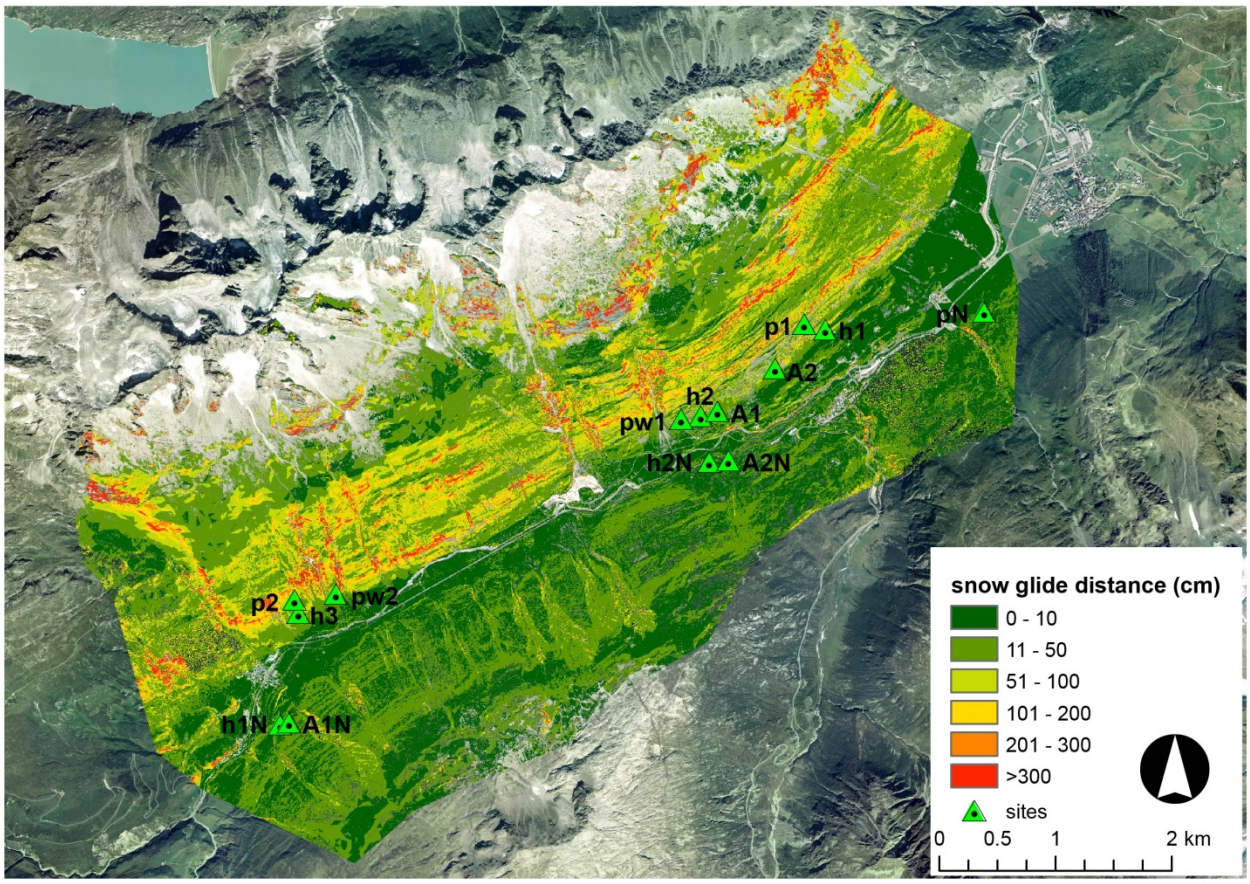

Fig. 8~~7~~ Map of the potential snow glide distance (m) modelled by SSGM.

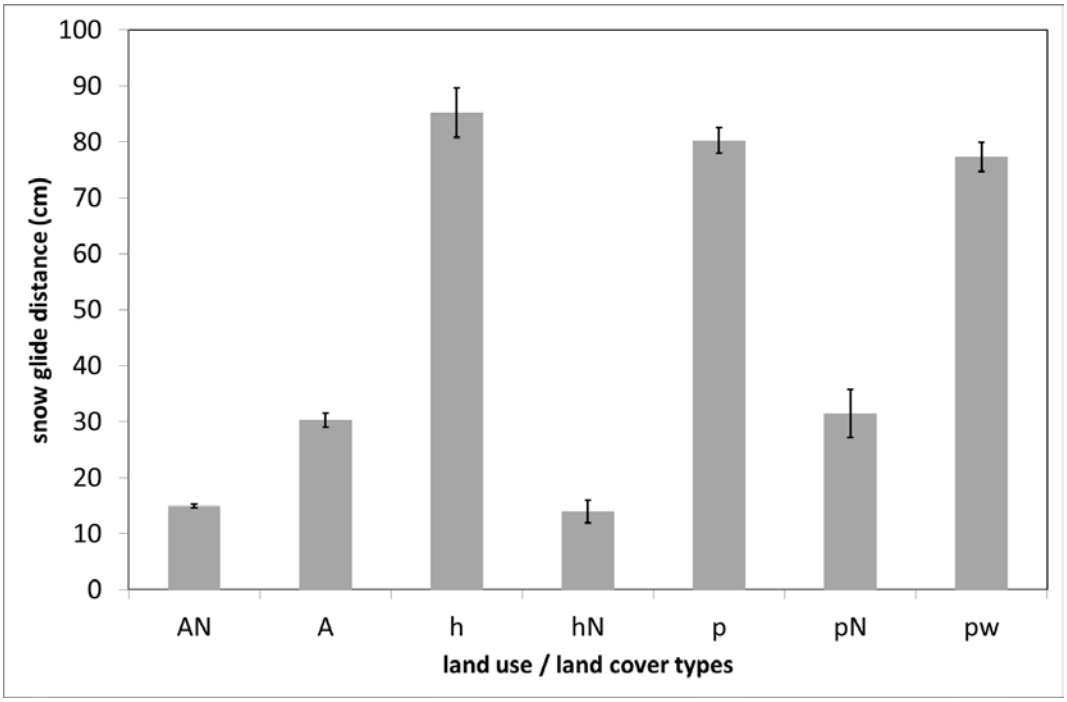

Fig. 9~~8~~ Modelled potential snow glide distances (using long-term average winter precipitation)) as mean for the whole catchment grouped by predominant land-use/cover types (hayfields (h), pastures (p), pastures with dwarf shrubs (pw), *Alnus viridis* sites (A)). N indicates the sites on the north facing slope. Error bars indicate the standard error of the mean.